Terra Antartica
2001, **8**(2), 79-86

TERRA ANTARTICA
AN ANTARCTIC EARTH SCIENCE JOURNAL

Cenozoic Tectonic History, Seismicity and Palaeoseismicity of the Antarctic Peninsula Pacific Margin

R.D. Larter

British Antarctic Survey, High Cross, Madingley Road, Cambridge CB3 0ET - UK
(rdla@pcmail.nerc-bas.ac.uk)

Abstract - Global earthquake catalogues do not record any earthquakes south of Bransfield Strait beneath the Antarctic Peninsula or its flanking continental shelves. Such low seismicity is consistent with neotectonic interpretations which show the area south of Bransfield Strait as part of the modern Antarctic plate. However, the magnitude distribution of earthquakes located in the wider region indicates that the threshold for location of events in this area was at least mb=4.5 before 1996. Plate tectonic reconstructions indicate that rapid subduction was taking place along the entire Pacific margin of the Antarctic Peninsula at the start of the Cenozoic era. By analogy with active subduction zones, and by reference to statistical relationships between seismicity parameters and other measurable parameters of modern subduction zones, it is inferred that this was an area of intense seismic activity at that time. On the same basis, well-constrained tectonic events affecting this margin imply that seismic activity decreased in stages during the Cenozoic era. Global catalogues list four earthquakes beneath the continental rise west of the Antarctic Peninsula. These occurred in oceanic lithosphere 16–49 Ma in age and do not appear to be associated with oceanic fracture zones. Harvard CMT focal mechanisms for two of these events indicate E–W and NE–SW shortening, and are interpreted as representing the regional tectonic stress field.

INTRODUCTION

At the present day the part of the Antarctic Peninsula Pacific margin south of Bransfield Strait is an area of low seismicity (Fig. 1). This is consistent with neotectonic interpretations which show that the area south of Bransfield Strait is all part of the modern Antarctic plate (Larter & Barker, 1991; Larter et al., 1997). In contrast, plate tectonic reconstructions indicate that at the start of the Cenozoic era rapid subduction was taking place along the entire Pacific margin of the Antarctic Peninsula (Fig. 2). By analogy with similar modern subduction zones the margin was probably an area of intense seismic activity at that time.

Estimation of the palaeoseismicity of a continental margin is relevant to interpretation of the sedimentary record from the continental rise. Morgenstern (1967)

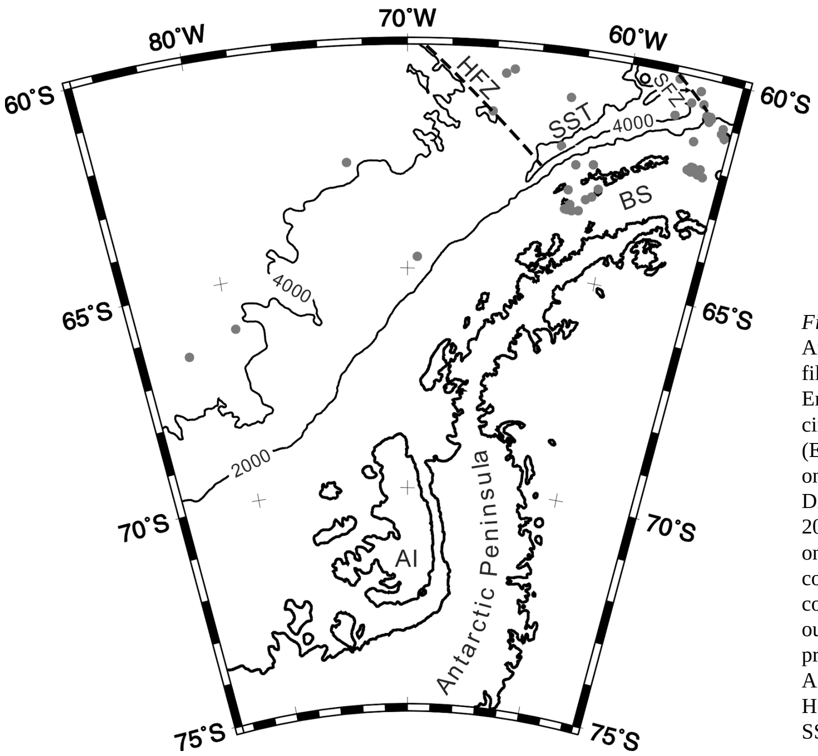

Fig. 1 - Earthquake epicentres (filled circles) in the Antarctic Peninsula region, from relocated hypocentre files for the period 1964–1998 (Engdahl et al., 1998; Engdahl, pers. comm., 2000). Also shown, as open circles, are the epicentres of two earlier earthquakes (Engdahl, pers. comm., 2000). Epicentres are overlaid on the Antarctic coastline from the SCAR Antarctic Digital Database (BAS, SPRI & WCMC, 1993) and 2000 m and 4000 m bathymetric contours, displayed on polar stereographic projection. The bathymetric contours in the central part of the map are based on data compiled by Rebesco et al. (1998) and the contours outside the area covered by these data are based on the predicted bathymetry data of Smith & Sandwell (1997). AI is Alexander Island, BS is Bransfield Strait, HFZ is Hero Fracture Zone, SFZ is Shackleton Fracture Zone, SST is South Shetland Trench.

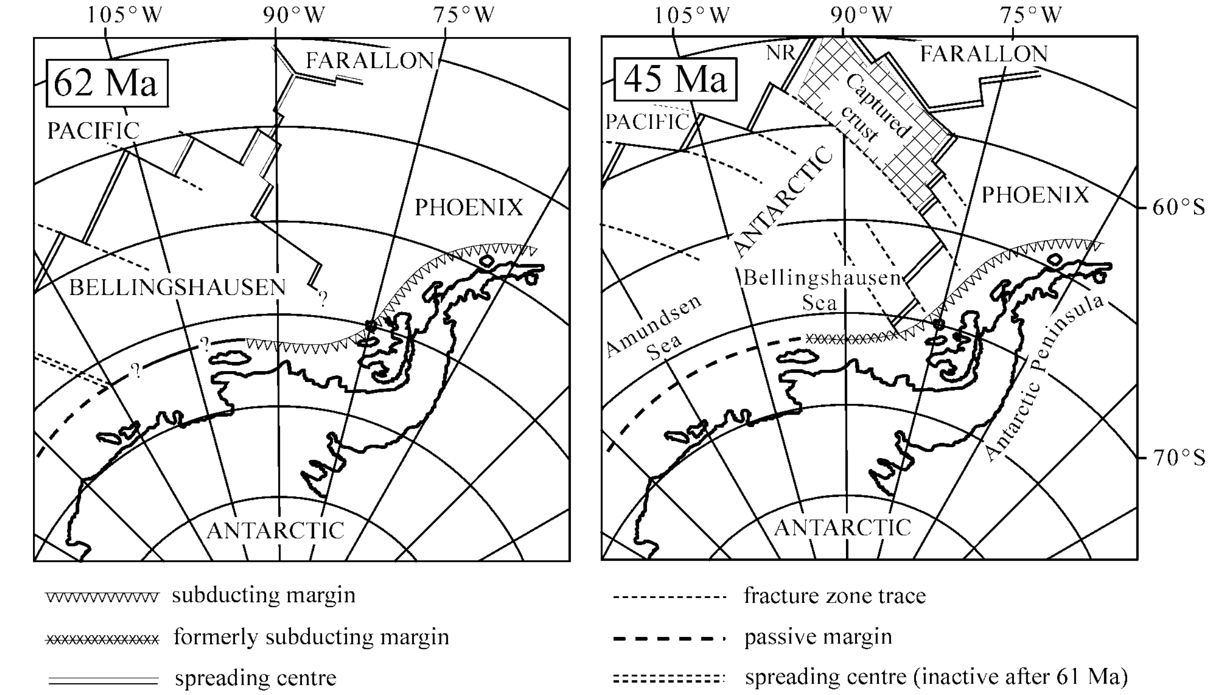

Fig. 2 - Reconstructions of the South Pacific in the Antarctic reference frame, assuming no relative motion between the component blocks of West Antarctica during the Cenozoic, based on data from Cande et al. (1982), Mayes et al. (1990) and Cande et al. (1995). The 62 Ma reconstruction approximately corresponds to the time that the Bellingshausen plate is thought to have been incorporated into the Antarctic plate (Cande et al., 1995). The Phoenix plate has also been referred to by some authors as the “Aluk” or “Drake” plate. NR is a new ridge formed by propagation of the Pacific–Antarctic ridge at about 47 Ma. After McCarron & Larter (1998).

accumulated data on submarine slumps caused by earthquakes and was able to show a correlation between submarine slumping and earthquakes with magnitudes greater than 6.5. Almagor & Wiseman (1977) concluded that even small earthquake-induced accelerations are sufficient to cause undrained slumping on moderate slopes. Therefore evidence of frequent slope failures may be expected on a continental margin which had a high level of seismicity, but a high frequency of failures is also likely to have resulted in individual mass wasting events involving smaller volumes than on margins where sediments were allowed to accumulate for longer periods without being disturbed.

This paper reviews the Cenozoic tectonic history of the Antarctic Peninsula region and, by analogy with active subduction zones elsewhere, considers how the main tectonic changes affected the seismicity of the Antarctic Peninsula Pacific margin. The information available in global earthquake catalogues for the small number of events reported beneath the continental rise west of the Antarctic Peninsula is also examined, and the relation of these events to the late Cenozoic tectonic history of the region is discussed.

TECTONIC HISTORY

At the beginning of the Cenozoic era the entire Pacific margin of the Antarctic Peninsula was an active plate margin (Larter et al., 1997; McCarron & Larter, 1998). The subducting oceanic lithosphere was part of the Phoenix plate (Larson & Chase, 1972), which some authors have referred to as the “Aluk” or “Drake” plate. The convergence direction is thought to have been approximately ESE, oblique to the general trend of the margin, and the convergence rate was >100 mm/yr. In early Tertiary time the convergence direction changed to SE, approximately perpendicular to most of the margin, but convergence rates remained >100 mm/yr (McCarron & Larter, 1998). It seems likely that this change in convergence direction was part of a general plate reorganization in the South Pacific which Cande et al. (1995) recognised as having taken place at magnetic reversal chron C27 time. This corresponds to 61 Ma on the magnetic reversal time scale of Cande & Kent (1995), which is used throughout this paper. The changes at chron C27 included the incorporation of the Bellingshausen plate into the Antarctic plate, and therefore Antarctic–Phoenix (ANT–PHO) sea-floor spreading probably also started at this time (Fig. 2). It has been inferred that initiation of ANT–PHO spreading during the chron C27 plate reorganization involved a westward ridge jump from a postulated former Bellingshausen–Phoenix spreading centre (Larter et al., 1999).

The onset of ANT–PHO spreading established an unusual tectonic situation in which the trailing flank of the spreading ridge and the overriding lithosphere at the Antarctic Peninsula Pacific margin were both part of the Antarctic Plate (Fig. 2). An implication of this tectonic setting is that the convergence rate at the margin must have equalled the full spreading rate at the ANT–PHO ridge. Only ocean floor formed on the trailing flank of the ridge is now preserved south of the Hero Fracture Zone (Fig. 1), but if symmetric spreading is assumed, the marine magnetic record of ANT–PHO spreading provides a record of convergence rates (Larter & Barker, 1991). The uncertainty resulting from the assumption of symmetric spreading is probably less than that associated with summation of plate rotations around a plate circuit, which is necessary to derive quantitative estimates of past convergence rates at all other convergent margins. The largest change in convergence rate indicated by marine magnetic data from the continental rise west of the Antarctic Peninsula occurred during chron C23 (52 Ma). At this time there was an abrupt decrease in half-spreading rate from 51 mm/yr to 21 mm/yr, implying a decrease in convergence rate from >100 mm/yr to 42 mm/yr (McCarron & Larter, 1998). After this abrupt decrease, convergence continued at intermediate rates, never again exceeding 70 mm/yr (Larter & Barker, 1991).

During the Tertiary period, subduction stopped along most of the margin as ridge-crest segments of the ANT–PHO spreading centre migrated into the trench (Larter & Barker, 1991; Larter et al., 1997). The unusual tectonic setting described above requires that as each ridge-crest segment arrived at the trench, subduction stopped along the opposing segment of the margin. Ridge-crest segments arrived first at the southwest part of the margin in Palaeocene or Eocene time, then progressively later toward the northeast. The first ridge-crest segment known to have migrated into the trench arrived at the part of the margin off southern Alexander Island (~83°W) during chron C20r (44 Ma) (McCarron & Larter, 1998). Other segments probably arrived earlier at the part of the margin farther west, but existing marine magnetic data are not adequate to confirm this. The last ridge-crest segment to arrive at the margin was the segment directly southwest of the Hero Fracture Zone, which entered the trench obliquely in latest Miocene and early Pliocene times (Larter & Barker, 1991).

Northeast of the Hero Fracture Zone, spreading stopped on the last remaining segments of the ANT–PHO ridge during the Pliocene, while they were still more than 250 km from the South Shetland Trench (Larter & Barker, 1991). Three dead ridge segments now lie in an en echelon pattern along approximately 66°W. Before spreading stopped, spreading rates on these segments decreased rapidly so that the convergence rate decreased from about 60 mm/yr during chron C3B (7 Ma) to <30 mm/yr by the start of chron C3n (5 Ma) (Larter & Barker, 1991; Maldonado et al., 1994). The start of this rapid decrease in spreading and convergence rates approximately coincides with the time at which spreading stopped in Drake Passage, to the east of the Shackleton Fracture Zone (Barker & Burrell, 1977).

Although spreading at the ANT–PHO ridge has stopped, shortening at the South Shetland Trench is continuing, accommodating active extension in Bransfield Strait (Maldonado et al., 1994; Kim et al., 1995; Barker & Austin, 1998). Teleseismically located earthquakes do not describe a Wadati-Benioff zone beneath the South Shetland Islands, but Pelayo & Wiens (1989) located two earthquakes at 35 and 55 km depth and suggested that underthrusting is largely aseismic as a consequence of the young age of the subducted slab and slow convergence rate. More recently, Ibáñez et al. (1997) have located 15 small-magnitude (Mw≤4.6) intermediate-focus (50–100 km depth) earthquakes beneath the South Shetland Islands and Bransfield Strait, which they interpret as originating from the subducted slab.

PALAEOSEISMICITY

The well-constrained Cenozoic tectonic history of the Antarctic Peninsula Pacific margin allows inferences about its palaeoseismicity to be made by analogy with active subduction zones elsewhere, and by reference to statistical relationships between seismicity parameters and other measurable parameters of modern subduction zones. Several stages in the Cenozoic history of the margin are closely analogous to different segments of the present day Pacific margin of South America.

A statistical analysis by Ruff & Kanamori (1980) revealed that the moment magnitude (Mw) of the largest earthquake within 21 modern subduction zones is significantly correlated with convergence rate and significantly inversely correlated with slab age. Sixty-four percent of the total variance in Mw was accounted for by these two variables. A slightly better fit was achieved when cumulative earthquake moment (Mw') was used as the independent variable instead of Mw. These relationships were re-examined by Jarrard (1986) through application of multiple regression analysis to 26 different subduction parameters, which included revised convergence rates and slab ages. The convergence rate estimates (Vc) in this analysis were based on results from Minster & Jordan (1978), excluded back-arc spreading (*i.e.* they were the rates between the subducting and major overriding plates), and were resolved perpendicular to the trench. The age of the ocean floor at the trench today was used as "slab age" (As). By multiple regression analysis Jarrard (1986) found that 62% of the total variance in Mw' was accounted for by the equation:

$$Mw' = 7.88 - 0.0096As + 0.177Vc \qquad (1)$$

where the units of As are millions of years and the units of Vc are cm/yr (Fig. 3). Furthermore, he found no significant correlation of regression residuals with any of the other possible independent variables considered in his analysis.

Notwithstanding the results of the statistical studies described above, it has been observed that the maximum earthquake magnitude and general level of seismicity are low in places where very young oceanic lithosphere is being subducted. Such places include the Cascadia subduction zone in western North America (Heaton & Kanamori, 1984), the southern Chile Trench (Nishenko, 1985), and the South Shetland Trench (Pelayo & Wiens, 1989). The explanation of this apparent contradiction may lie in the fact that the data used by Ruff & Kanamori (1980) and by Jarrard (1986) to determine correlations between Mw, Mw', Vc and As only included one subduction zone

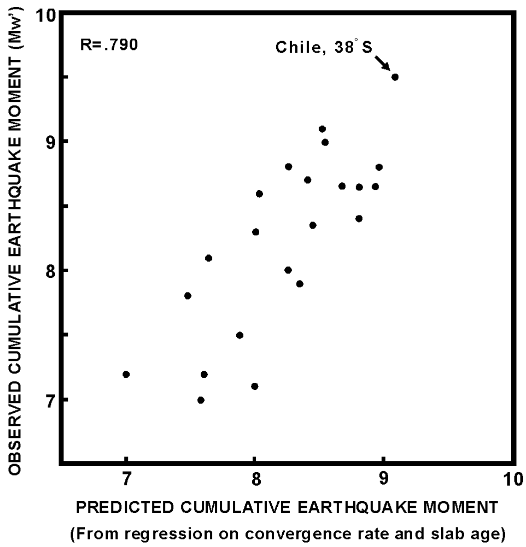

Fig. 3 - Cross plot of cumulative earthquake moment (*Mw'*) versus predicted *Mw'*, based on a regression equation in which slab age and convergence rate are the independent variables (see text for details). Redrawn after Jarrard (1986).

where the age of the lithosphere at the trench was estimated to be less than 20 Ma. Therefore these analyses do not preclude the possibility that the relationships of Mw and Mw' to As could be non-linear, and could even change from inverse to positive correlations for very young slab ages.

At the start of the Cenozoic, most of the oceanic lithosphere subducting beneath the Antarctic Peninsula had been formed at the Pacific–Phoenix ridge at half spreading rates > 50 mm/yr (Mayes et al., 1990; McCarron & Larter, 1998). The reconstruction for 62 Ma in figure 2 shows that at this time the remaining segments of the Pacific–Phoenix ridge were about 1200 km from the Antarctic Peninsula margin. Therefore most of the oceanic lithosphere entering the trench at this time was probably 20–30 m.y. old. Convergence rates at the trench are estimated to have remained > 100 mm/yr from Late Cretaceous time until chron C23 (52 Ma), despite the major plate reorganization assigned to chron C27 (61 Ma). Given a slab age of 25 m.y. and a convergence rate of 100 mm/yr, equation (1) gives a predicted Mw' of 9.4, which is greater than that for any of the modern subduction zones considered in the analysis by Jarrard (1986). The closest modern analogy is the Chile subduction zone at 38°S, for which Jarrard (1986) used a slab age value of 26 Ma and a convergence rate of 82 mm/yr. These parameters give a predicted Mw' of 9.1, which compares well with the observed Mw' of 9.5, both figures being greater than those for any other subduction zone in the analysis. In the interval 1973–1997 the U.S. Geological Survey's National Earthquake Information Center (NEIC) Preliminary Determination of Epicenters (PDE) database includes more than 500 earthquakes with body-wave magnitudes (mb)≥5.0 beneath western South America between 30°S–40°S. There is every reason to suspect that the Antarctic Peninsula Pacific margin was just as seismically active, if not more active, at the start of the Cenozoic era. In addition to typical subduction-related activity, oblique convergence is likely to have enhanced seismicity by causing strike-slip deformation in the forearc and arc, as observed in many obliquely convergent plate margins, including central Chile (Forsythe & Nelson, 1985; Jarrard, 1986).

The abrupt decrease in Phoenix–Antarctic convergence rate from >100 mm/yr to 42 mm/yr during chron C23 (52 Ma) would, according to equation (1), have resulted in a concomitant decrease in Mw'. From marine magnetic anomaly data (Cande et al., 1982; McCarron & Larter, 1998) I estimate that ANT–PHO ridge segments were between 150 km and 450 km from the margin at this time, while farther north Pacific–Phoenix ridge segments were up to 800–900 km from the margin. The half-spreading rate at the ANT–PHO ridge from the time of its inception during chron C27 (61 Ma) until chron C23 averaged 51 mm/yr (McCarron & Larter, 1998). Therefore the oceanic lithosphere entering the trench southeast of the ANT–PHO ridge segments during chron C23 ranged from about 3 m.y. to about 9 m.y. in age. For the Pacific–Phoenix ridge Cande et al. (1982) estimated early Tertiary half-spreading rates as high as 113 mm/yr. However, recalculation of these rates using the magnetic reversal time scale of Cande & Kent (1995) results in an average Pacific–Phoenix half-spreading rate between chron C27 and chron C23 of 81 mm/yr. Therefore the oceanic lithosphere entering the trench southeast of the Pacific–Phoenix ridge segments during chron C23 is estimated to have been 10–11 m.y. old. Given a convergence rate of 42 mm/yr and slab ages ranging from 3 m.y. to 11 m.y., equation (1) gives predicted Mw' values between 8.5 and 8.6. This is a substantial decrease from the value calculated for 62 Ma. However, the observations mentioned above, of relatively low seismicity at margins where very young oceanic lithosphere is being subducted today, suggest that these values may still give an exaggerated impression of the level of seismicity following the chron C23 (52 Ma) decrease in convergence rate.

In the last few million years before each ANT–PHO ridge-crest segment migrated into the trench, progressively younger oceanic lithosphere entered the subduction zone ahead of the ridge. In the light of the relatively low levels of seismicity observed where very young oceanic lithosphere is being subducted today, especially where convergence is slow, I suggest that seismicity probably decreased along the opposing segment of the margin as each ridge segment approached the trench. The part of the Chilean margin directly north of where the Chile Ridge (Antarctic–Nazca spreading centre) is being subducted provides the best modern analogue to this situation. The Chile Ridge meets the Chile Trench at about 46°30'S, and the oceanic lithosphere formed at the Chile Ridge which is entering the trench between this triple junction and 44°S is less than 7 Ma in age (Cande et al., 1987). The Nazca–South America convergence rate in this area is 84 mm/yr (DeMets et al., 1990). In the interval 1973–1997 the NEIC PDE database includes only 20 earthquakes with mb≥5.0 beneath western South America between 44°S–46°S, and 9 of these were part of a swarm which occurred during a single day in 1991. The largest of these events has a surface wave magnitude (Ms) of 5.7. When oceanic lithosphere of similar age was being subducted at the Antarctic Peninsula Pacific margin the level of seismicity is expected to have been even lower as a consequence of the slower convergence rates.

The arrival of each ridge-crest segment at the Antarctic Peninsula Pacific margin resulted in the termination of subduction along the affected segment of margin. Once subduction stopped, seismic activity probably decreased quickly to a level similar to normal intraplate activity. The level of seismic activity after such an event would certainly have been lower than the level of modern seismicity south of the Chile Trench triple junction, where slow subduction has continued following migration of the Chile Ridge into the trench. Young oceanic lithosphere that is part of the Antarctic plate is now being subducted at the southern Chile Trench at a rate of 20 mm/yr (DeMets et al., 1990). Between 47°S–49°S the Chile Ridge entered the trench between 3 Ma and 10 Ma (Cande et al., 1987). In the interval 1973–1997 the NEIC PDE database includes only 5 earthquakes with mb≥5.0 beneath western South America between 47°S–49°S, and for the largest of these events Ms=5.3.

MODERN SEISMICITY

Today the Antarctic Peninsula and flanking continental shelves south of 63°30'S appear to be entirely passive. Global earthquake catalogues compiled since the inception of the World-Wide Standard Seismograph Network in 1963 do not record any earthquakes south of this latitude beneath the Peninsula or flanking shelf areas. However, the mb distribution of earthquakes in the NEIC PDE database which occurred in the Antarctic Peninsula and South Shetland Islands area since 1973 suggests that the threshold for location of events in this region from teleseismic data was greater than mb=4.5 until the middle of the present decade (Fig. 4). Five of the six events detected in the region with mb<4.5 have occurred since 1995.

Post-1963 global catalogues do record four earthquakes in oceanic lithosphere beneath the continental rise west of

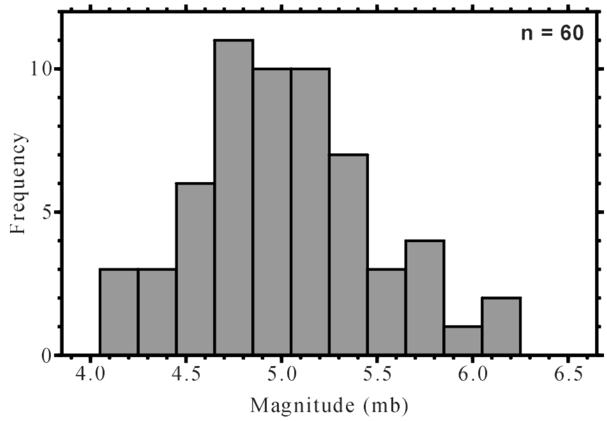

Fig. 4 - Histogram of body wave magnitudes of all earthquakes in the U.S. Geological Survey's National Earthquake Information Centre Preliminary Determination of Epicenters database which occurred in the area shown in figure 1 from 1973–1999.

the Antarctic Peninsula and southwest of the Hero Fracture Zone (Fig. 5). In the International Seismological Centre (ISC) catalogue the magnitudes (mb) of these events are recorded as 6.1, 5.1, 4.9 and 4.4. The events do not appear to be associated with oceanic fracture zones, with the possible exception of event 4 (Tab. 1, Fig. 5). Hypocentral depth estimates based on studies using depth phases (Engdahl et al., 1998; Engdahl, pers. comm. 2000) or body waveform inversion (Wiens & Stein, 1983) are available for 3 of the events and are in the range 12–28 km (Tab. 1). The age of the oceanic lithosphere in which these earthquakes occurred has been determined by overlaying the epicentre locations (Engdahl et al., 1998; Engdahl, pers. comm., 2000) on interpretations of marine magnetic data (Larter & Barker, 1991; Larter et al., 1999). The resulting ages range from 16 Ma to 49 Ma (Tab. 1).

The Harvard centroid moment tensor (CMT) catalogue provides focal mechanisms for events 1 and 3 (Fig. 5), which occurred in 49 Ma and 31 Ma lithosphere, respectively (Tab. 1). Both are thrust mechanisms, the one for event 1 indicating approximately E–W shortening and the one for event 3 indicating approximately NE–SW shortening. Another focal mechanism for event 1 was produced by Okal (1980) using body- and surface-wave first motion data, but the result is almost identical to the

Tab. 1 - Magnitudes, depth estimates and crustal ages for earthquakes beneath the Antarctic Peninsula continental rise. Epicentre locations are shown in figure 5. Body wave magnitudes (*mb*) and the *Ms* estimate for event 2 are from the *ISC Bulletin*. The other magnitude values are from the Harvard CMT catalogue. Depth estimates in "ISC" column are from *ISC Bulletin*, those in "EHB" column are from Engdahl et al. (1998), revised by Engdahl (pers. comm., 2000), with the number of depth phase observations in parentheses. Depth estimates in the "Okal (80)" and "W&S (83)" columns are from Okal (1980) and Wiens & Stein (1983), respectively. Age of crust is determined from the position of epicentres in relation to interpretations of marine magnetic data (Larter and Barker, 1991; Larter et al., 1999), using the magnetic reversal time scale of Cande and Kent (1995).

Event	**Magnitudes**			**Depth estimates (km)**				**Age of crust (Ma)**
	mb	***Ms***	***Mw***	**ISC**	**EHB**	**Okal (80)**	**W&S (83)**	
1	6.1	6.2	6.3	31	27.5 (7)	35	15	49
2	5.1	4.3		10	25.0 (1)			43
3	4.9		5.0	10	15.0 (0)			31
4	4.4			20	12.7 (9)			16

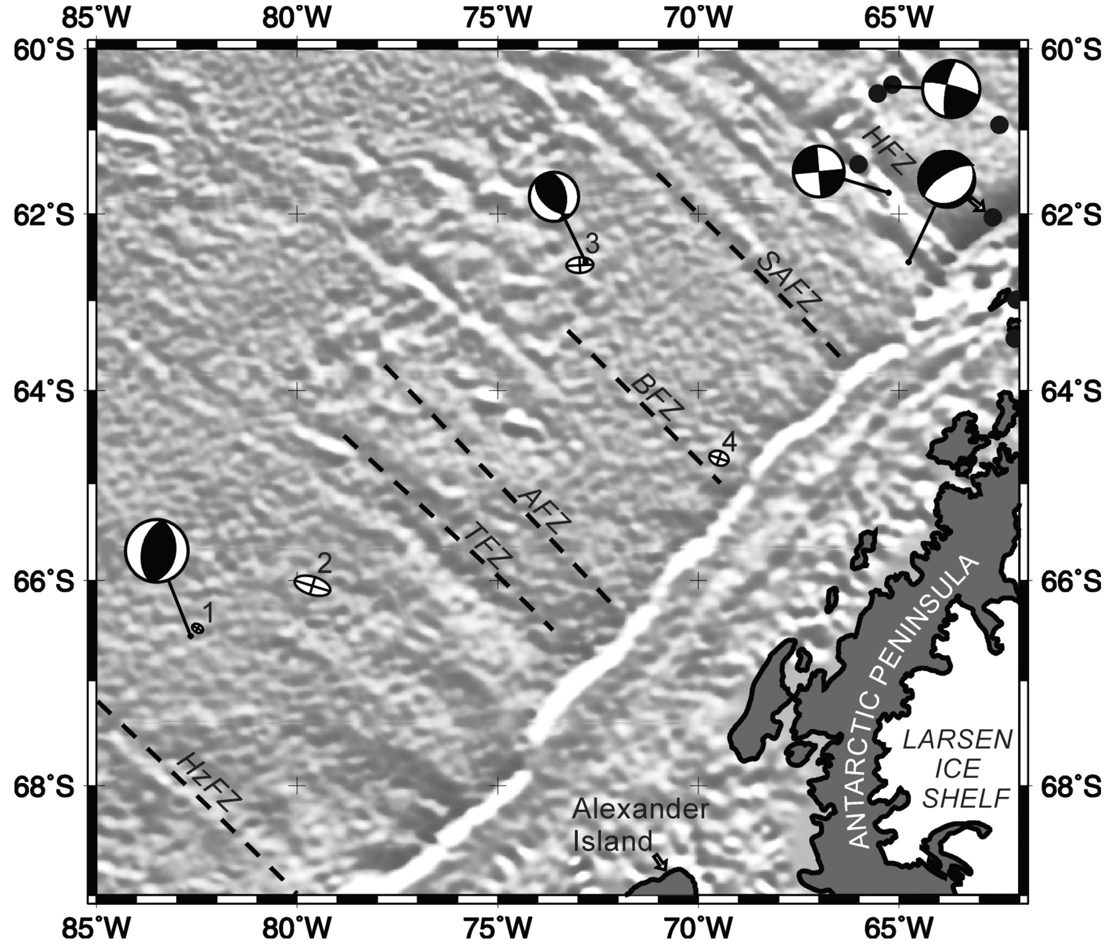

Fig. 5 - Earthquake epicentres from relocated hypocentre files for the period 1964–1998 and Harvard CMT focal mechanisms on the Antarctic Peninsula Pacific margin, overlaid on Mercator projection of the free-air gravity anomaly field derived from satellite altimetry data (Sandwell & Smith, 1997). 90% confidence ellipses are shown for the epicentre locations of the four events listed in Table 1 (Engdahl, pers. comm., 2000); other epicentres are shown as filled circles (Engdahl et al., 1998). Focal mechanism radius is proportional to magnitude (*Mw*). Focal mechanisms all relate to the same event as the nearest epicentre, except for one focal mechanism for an event in the South Shetland Trench where the associated epicentre is indicated by an arrow. The gravity anomaly field is illuminated from NNE: positive anomalies and NNE-dipping gradients appear light; negative anomalies and SSW-dipping gradients appear dark. The positions of oceanic fracture zones interpreted from marine magnetic and seismic data (Larter & Barker, 1991; Larter et al., 1999) are shown as dashed lines. The Hero Fracture Zone (HFZ) and other fracture zones parallel to it near the northeastern corner of the map are not marked by dashed lines as they are clearly evident in the gravity field. Numbers annotated next to epicentres on the continental rise west of the Antarctic Peninsula are the event numbers which appear in Table 1. Antarctic coastline is from the SCAR Antarctic Digital Database (BAS, SPRI & WCMC, 1993). AFZ is Adelaide Fracture Zone, BFZ is Biscoe Fracture Zone, HzFZ is Heezen Fracture Zone, SAFZ is South Anvers Fracture Zone, TFZ is Tula Fracture Zone.

CMT mechanism. Okal (1980) also estimated the focal depth of this earthquake to be 35 km using a waveform modelling method, and calculated the seismic moment to be (4.4 ± 1.5) x 10^{25} dyn cm, which is equivalent to Mw=6.4. The Harvard CMT catalogue gives a slightly smaller seismic moment for this earthquake: 3.15 x 10^{25} dyn cm (Mw=6.3) (Tab. 1). Earthquakes with seismic moments greater than 10^{25} dyn cm are rare in oceanic lithosphere older than 15 Ma (Bergman & Solomon, 1984), so this is an exceptionally large earthquake to have occurred in 49 Ma lithosphere.

Oceanic intraplate earthquakes occur most frequently in oceanic lithosphere 30 Ma or less in age (Wiens & Stein, 1983, 1984). This excess seismicity in young oceanic lithosphere has been attributed to either thermoelastic stress or near-ridge stress concentrations due to local heterogeneities in the spreading process (Wiens & Stein, 1983; Bratt et al., 1985). Focal mechanisms of earthquakes in older oceanic lithosphere generally indicate compressional stress and, particularly where they are free from local biasing effects of pre-existing fault zones and large bathymetric relief, are thought to be representative of the long-wavelength tectonic stress field (Bergman & Solomon, 1980). Therefore the two focal mechanisms for earthquakes beneath the continental rise west of the Antarctic Peninsula suggest regional E–W to NE–SW compression, although several more focal mechanisms in the same area are needed before this observation can be considered statistically significant. The observation is, however, consistent with other focal mechanisms to the northeast of this area, and with some models for the cessation of spreading and the neotectonic regime on the

ANT-PHO ridge. A tentative focal mechanism determined by Forsyth (1975) indicates NE-SW directed reverse faulting near the central ANT–PHO dead ridge segment, while two CMT focal mechanisms indicate strike-slip faulting near the southern ANT–PHO dead ridge segment and near the Hero Fracture Zone (Fig. 5). In the case of both CMT mechanisms the strikes of the possible strike-slip fault planes are oblique to the tectonic lineaments they are associated with, a pattern of faulting which is consistent with a compressional stress regime.

A present-day plate motion model for the Scotia Sea region derived from earthquake slip vectors and other data by Pelayo & Wiens (1989) predicts E–W compression on the Shackleton Fracture Zone (Fig. 1). The scattered seismicity along the ANT–PHO (“Aluk”) ridge was interpreted by Pelayo & Wiens (1989) as a reflection of diffuse deformation of the area to the west of the Shackleton Fracture Zone in response to this compression. It has also been proposed that the development of E–W compression in this region was the cause of slowing and eventual stoppage of spreading on the ANT–PHO ridge, through imposition of compressive stress on the long strike-slip boundaries of the Phoenix plate, the Shackleton and Hero fracture zones (Barker & Dalziel, 1983). Calculations of the approximate slab pull and ridge push forces operating on the Phoenix plate since the early Oligocene by Larter & Barker (1991) did not reveal any change in plate driving forces that could have caused either the rapid decrease in ANT–PHO spreading rates which began at the end of chron C3B (7 Ma), or the eventual stoppage of spreading during the Pliocene. On this basis, Larter & Barker (1991) concluded that the cause for slowing and stoppage of spreading must have involved an increased resistive force, and suggested the most likely cause was increased compressive stress at the Shackleton and Hero fracture zones, resulting from changes in the mode of Scotia Sea evolution to the east. The regional stress regime inferred from earthquake focal mechanisms in the region is consistent with this hypothesis.

CONCLUSIONS

1) Global earthquake catalogues do not record any events south of 63°30' S beneath the Antarctic Peninsula or its flanking continental shelves. Before 1996, however, the magnitude threshold for location of events in this region was at least mb=4.5.
2) Plate tectonic reconstructions suggest that the Antarctic Peninsula Pacific margin was an area of intense seismic activity at the start of the Cenozoic era.
3) Seismic activity at this margin probably decreased in stages during the Cenozoic era as a result of:
   a. an abrupt decrease in convergence rate during chron C23 (52 Ma),
   b. very young oceanic lithosphere entering the trench ahead of each ANT–PHO ridge-crest segment, and
   c. progressive termination of subduction from southwest to northeast as ANT–PHO ridge-crest segments migrated into the trench.
4) Global earthquake catalogues list four earthquakes beneath the continental rise west of the Antarctic Peninsula and southwest of the Hero Fracture Zone, in oceanic lithosphere 16–49 Ma old.
5) Harvard CMT focal mechanisms are available for two of the events which occurred beneath the continental rise, and these indicate E–W and NE–SW shortening. Most thrust earthquakes in oceanic lithosphere of this age are thought to be representative of the regional tectonic stress field. Therefore these focal mechanisms appear to suggest regional E–W to NE–SW compression, although several more focal mechanisms in the same area are needed before this observation can be considered to be statistically significant. The observation is, however, consistent with a present-day plate motion model which predicts E–W compression across the Shackleton Fracture Zone, and with the hypothesis that ANT–PHO spreading stopped because of imposition of compressive stress on the long strike-slip boundaries of the Phoenix plate.

ACKNOWLEDGEMENTS - I am grateful to the Organizing Committee of the workshop on ‘Broad-Band Seismic Observations and the Geodynamics of the Scotia Sea Region, Antarctica’ for arranging a stimulating meeting, and to workshop participants for useful discussions. I also thank Carlo Doglioni and Bob Engdahl for helpful reviews. Bob Engdahl further improved the paper by providing data describing two historical events and recomputed hypocentre data, including 90% confidence ellipses, for the four events in table 1.

REFERENCES

Almagor G. & Wiseman G., 1977. Analysis of submarine slumping in the continental slope off the southern coast of Israel. *Marine Geotechnology*, **2**, 349-388.

Barker D.H.N. & Austin J.A., 1998. Rift propagation, detachment faulting, and associated magmatism in Bransfield Strait, Antarctic Peninsula. *J. Geophys. Res.*, **103**, 24017-24043.

Barker P.F. & Burrell J., 1977. The opening of Drake Passage. *Mar. Geol.*, **25**, 15-34.

Barker P.F. & Dalziel I.W.D., 1983. Progress in geodynamics in the Scotia Arc region. In: Cabre R. (ed.), *Geodynamics of the Eastern Pacific Region, Caribbean and Scotia Arcs, AGU Geodynamics Series*, **9**, 137-170.

BAS, SPRI & WCDC, 1993. Antarctic Digital Database User’s Guide and Reference Manual, Scientific Committee on Antarctic Research, Cambridge, xi + 156 pp.

Bergman E.A. & Solomom S.C., 1980. Oceanic intraplate earthquakes: implications for local and regional intraplate stress. *J. Geophys. Res.*, **85**, 5389-5410.

Bergman E.A. & Solomon S.C., 1984. Source mechanisms of earthquakes near mid-ocean ridges from body waveform inversion: implications for the early evolution of oceanic lithosphere. *J. Geophys. Res.*, **89**, 11415-11441.

Bratt S.R., Bergmann E.A. & Solomon S., 1985. Thermoelastic stress: how important as a cause of young earthquakes in young oceanic lithosphere? *J. Geophys. Res.*, **90**, 10249-10260.

Cande S.C. & Kent D.V., 1995. Revised calibration of the geomagnetic polarity timescale for the Late Cretaceous and Cenozoic. *J. Geophys. Res*., **100**, 6093-6095.

Cande S.C., Herron E.M. & Hall B.R., 1982. The early Cenozoic tectonic history of the southeast Pacific. *Earth Planet. Sci. Lett*., **57**, 63-74.

Cande S.C., Leslie, R.B., Parra, J.C. & Hobart, M., 1987. Interaction between the Chile Ridge and Chile Trench: geophysical and geothermal evidence. *J. Geophys. Res.*, **92**, 495-520.

Cande S.C., Raymond, C.A., Stock, J. & Haxby, W.F., 1995. Geophysics of the Pitman Fracture Zone and Pacific–Antarctic plate motions during the Cenozoic. *Science*, **270**, 947-953.

DeMets C., Gordon, R.G., Argus, D.F. & Stein, S., 1990. Current plate motions. *Geophys. J. Int.*, **101**, 425-478.

Engdahl R.E., van der Hilst R. & Buland R., 1998. Global teleseismic earthquake relocation with improved travel times and procedures for depth determination. *Bull. Seismol. Soc. Am.*, **88**, 722-743.

Forsyth D.W., 1975. Fault plane solutions and tectonics of the South Atlantic and Scotia Sea. *J. Geophys. Res.*, **80**, 1429-1443.

Forsythe R.D. & Nelson E.P., 1985. Geological manifestations of ridge collision: evidence from the Golfo de Penas–Taitao Basin, southern Chile. *Tectonics*, **4**, 477-495.

Heaton T.H. & Kanamori H., 1984. Seismic potential associated with subduction in the northwestern United States. *Bull. Seismol. Soc. Am.*, **74**, 933-941.

Ibáñez J.M., Morales J., Alguacil G., Almendros J., Ortiz R. & Del Pezzo E., 1997. Intermediate-focus earthquakes under South Shetland Islands (Antarctica). *Geophys. Res. Lett.*, **24**, 531-534.

Jarrard R.D., 1986. Relations among subduction parameters. *Rev. Geophys.*, **24**, 217-284.

Kim Y., Kim H.-S., Larter R.D., Camerlenghi A., Gambôa L.A.P. & Rudowski S., 1995. Tectonic deformation in the upper crust and sediments at the South Shetland Trench. In: Cooper A.K., Barker P.F. & Brancolini G. (eds.), *Geology and seismic stratigraphy of the Antarctic margin, Part 1*, AGU Antarctic Research Series, **68**, 157-166.

Larson R.L. & Chase C.G., 1972. Late Mesozoic evolution of the western Pacific Ocean. *Geol. Soc. Am. Bull.*, **83**, 3627-3644.

Larter R.D. & Barker P.F., 1991. Effects of ridge crest–trench interaction on Antarctic–Phoenix spreading: forces on a young subducting plate. *J. Geophys. Res.*, **96**, 19583-19607.

Larter R.D., Rebesco M., Vanneste L.E., Gambôa L.A.P. & Barker P.F., 1997. Cenozoic tectonic, sedimentary and glacial history of the continental shelf west of Graham Land, Antarctic Peninsula. In: Cooper A.K. & Barker P.F. (eds.), *Geology and seismic stratigraphy of the Antarctic margin, Part 2*, AGU Antarctic Research Series, **71**, 1-27.

Larter R.D., Cunningham A.P., Barker P.F., Gohl K. & Nitsche F.O., 1999. Structure and tectonic evolution of the West Antarctic continental margin and Bellingshausen Sea. *Korean Journal of Polar Research*, **10**, 125-133.

Maldonado A., Larter R.D. & Aldaya F., 1994. Forearc tectonic evolution of the South Shetland margin, Antarctic Peninsula. *Tectonics*, **13**, 1345-1370.

Mayes C.L., Lawver L.A. & Sandwell D.T., 1990. Tectonic history and new isochron chart of the South Pacific. *J. Geophys. Res.*, **95**, 8543-8567.

McCarron J.J. & Larter R.D., 1998. Late Cretaceous to early Tertiary subduction history of the Antarctic Peninsula. *J. Geol. Soc. London*, **155**, 255-268.

Minster J.B. & Jordan, T.H., 1978. Present-day plate motions. *J. Geophys. Res.*, **83**, 5331-5354.

Morgenstern N.M., 1967. Submarine slumping and the initiation of turbidity currents. In: Richards A.F. (ed.), Marine Geotechnique, University of Illinois Press, Urbana, Illinois, pp. 189-220.

Nishenko S.P., 1985. Seismic potential for large and great interplate earthquakes along the Chilean and southern Peruvian margins of South America: a quantitative reappraisal. *J. Geophys. Res.*, **90**, 3589-3615.

Okal E.A., 1980. The Bellingshausen Sea earthquake of February 5, 1977:evidence for ridge-generated compression in the Antarctic plate. *Earth Planet. Sci. Lett.*, **46**, 306-310.

Pelayo A.M. & Wiens D.A., 1989. Seismotectonics and relative plate motions in the Scotia Sea region. *J. Geophys. Res.*, **94**, 7293-7320.

Rebesco M., Camerlenghi A. & Zanolla C., 1998. Bathymetry and morphogenesis of the continental margin west of the Antarctic Peninsula. *Terra Antartica*, **5**, 715-725.

Ruff L., & Kanamori H., 1980. Seismicity and the subduction process. *Phys. Earth Planet. Inter.*, **23**, 240-252.

Sandwell D.T. & Smith W.H.F., 1997. Marine gravity anomaly from Geosat and ERS 1 satellite altimetry. *J. Geophys. Res.*, **102**, 10039-10054.

Smith W.H.F. & Sandwell D.T., 1997. Global sea floor topography from satellite altimetry and ship depth soundings. *Science*, **277**, 1956-1962.

Wiens D.A. & Stein S., 1983. Age dependence of oceanic intraplate seismicity and implications for lithospheric evolution. *J. Geophys. Res.*, **88**, 6455-6468.

Wiens D.A. & Stein S., 1984. Intraplate seismicity and stress in young oceanic lithosphere. *J. Geophys. Res.*, **89**, 11442-11464.